PAPER

Check for updates

Sulfonated biochar catalyst derived from eucalyptus tree shed bark: synthesis, characterization and its evaluation in oleic acid esterification

Adeyinka S. Yusuff, [ID] *[a] Kudirat A. Thompson-Yusuff[b] and Jyoti Porwal[c]

Herein, fatty acid (oleic acid, OA) was upgraded to fatty acid methyl ester (FAME) *via* esterification reaction using sulfonated biochar obtained from eucalyptus tree shed bark as solid acid catalyst. Under the optimal esterification conditions (*i.e.*, at 65 °C for 2 h using a methanol/OA molar ratio of 10 : 1 with a catalyst dosage of 4 wt%), the FAME yield was 97.05 $\pm$ 0.28% when a solid acid catalyst prepared by loading 6 g of *p*-Toluenesulfonic acid (*p*-TSA) on 2 g of activated biochar (*p*-TSA$_3$/ABC) was used. The remarkable performance of the *p*-TSA$_3$/ABC could be attributed to its high acidity (468.8 μmol g^{-1}) and dominance of the SO$_3$H acid site on the catalyst surface. Experimental findings showed that the *p*-TSA$_3$/ABC was relatively stable due to its highly functionalized structure. The catalyst was recycled for five successive cycles and exhibited no dramatic decrease in catalytic activity.

1. Introduction

Esterification of organic acid and alcohol is known to be the basic reaction process for producing valuable materials in some manufacturing industries.[1] Also, the esterification process is employed as one of the reaction steps for converting feedstock with high free fatty acid (FFA) to biodiesel. Generally, esterification of low-quality feedstock or fatty acids with simple alcohol requires a solid or liquid catalyst in order to enhance the reaction rate and product yield.

Basically, acid catalysts are often used to catalyze the esterification reaction as a base catalyst could react with FFA to form undesired products through saponification and, as a result, lower the desired product yield and quality.[2] Research has shown that the application of liquid acid (homogeneous) catalyst in the synthesis of methyl esters from low-grade feedstocks requires excess catalyst amount and a larger reactor.[3–5] More so, reusability of the spent catalyst is impossible since the liquid catalyst would mix with a liquid reactant, thus resulting in wastewater generation as washing is required to strip off the acid catalyst from the product.[2] In contrast, the utilization of solid acid (heterogeneous) catalysts could reduce the incidence of corrosion, guarantee an ecofriendly environment and facile processes, and ensure catalyst reusability.

Overall, mineral acids, such as H$_2$SO$_4$ and HF, have been impregnated onto support materials in order to improve the acidic strength, activity and stability of the resulting solid acid catalysts in heterogeneous acid-catalyzed reaction.[6,7] However, most synthesized solid catalysts reported are costly and require a tedious preparation process.[2,8] Although H$_2$SO$_4$ impregnated carbon-based catalysts have been proved to be effective in the esterification of FFA,[9,10] utilization of H$_2$SO$_4$ as sulfonating agent for sulfonated catalyst preparation could result in corrosion if high pressure withstanding reactor is not used and requires special precautionary measures.[11,12] Therefore, there is the need to search for alternative sulfonating agents that are less corrosive, have low vapor pressure and have better catalytic performance. In this regard, *para*-toluene sulfonic acid (*p*-TSA) has been considered as a sulfonating agent with those qualities mentioned above.[13] It is an aromatic ring connected to a long alkyl chain which endows it with an amphiphilic nature.[2]

Most sulfonated carbon-based catalysts have been synthesized *via p*-TSA treatment. Zhang *et al.*[14] synthesized a novel sulfonated carbon-based material from *p*-TSA and glucose and applied it as a solid acid catalyst for esterification of FFA. Also, biodiesel was produced from high acid value *Jatropha* oil using solid acid catalyst obtained from impregnation of *p*-TSA on lignin[15]. Furthermore, Russo *et al.*[16] utilized a –SO$_3$H functionalized carbon-silica composite derived *via p*-TSA treatment followed by H$_2$SO$_4$ sulfonation for biomass conversion and concluded that the *p*-TSA was able to prevent the damaging corrosion. Dechakhumwat *et al.*[2] utilized corncob residue to synthesize heterogeneous acid catalyst using *p*-TSA as

[a]Department of Chemical and Petroleum Engineering, College of Engineering, Afe Babalola University, Ado-Ekiti, Nigeria. E-mail: yusuffas@abuad.edu.ng

[b]Department of Chemical and Polymer Engineering, Faculty of Engineering, Lagos State University, Epe Campus, Epe, Nigeria

[c]Material Resource Efficiency Division, CSIR-Indian Institute of Petroleum, Dehradun, India

a sulfonating agent for esterification of oleic with methanol to produce biodiesel.

The preparation of sulfonated carbon-based catalysts from biomass or waste could reduce the biodiesel production cost, guarantee process sustainability and serve as a mitigation measure for waste management. Some of the biomass or waste materials that have been used as sulfonated catalyst supports include corncob,[2] coffee residue,[1] palm kernel shells,[12] sweet potato peel,[17] rice husk,[18,19] waste orange peel,[20] coconut meal residue,[21] hyacinth leaves,[22] Cacao shell,[23] lignin,[15] Willow catkins,[24] cotton stalk,[25] tomato peel waste,[26] hazelnut shells,[27] hura crepitans seed pod,[28] waste pomelo peel,[29] sugarcane bagasse[30] and so on. Most of these materials are carbonaceous materials and could serve as sources of biochar.

Biochar is a carbon-rich material derived *via* pyrolysis or degasification of organic material at high temperature (usually 300–650 °C) under little or no oxygen in order to avoid combustion.[12,31] Research has shown that biochar, as catalyst support, is effective for developing solid acid catalysts due to its good textural properties, better thermal stability and numerous functional groups.[32] However, by comparing the commercial activated carbon with the biochar, there is the need to improve the surface properties of the latter. Synthesis of activated or modified biochar *via* chemical activation using zinc chloride as activating agent can result in modified biochar with high surface area, abundant surface functional groups, porous structure and high adsorption capacity.[32,33] Ngaosuwan *et al.*[1] had used $ZnCl_2$-modified biochar obtained from the coffee residue as a support for the sulfonated carbon-based catalyst for esterification reaction. As a result, it is worthwhile to investigate and modify other biomass materials as catalyst sources for the esterification reaction. Eucalyptus trees grow quickly and are widely available in most parts of the world, producing large quantities of bark that is discarded as waste.[34] Furthermore, eucalyptus tree shed bark, which contains a higher percentage of organic matter than other plant-based biomasses, is abundant and can be used as a starting material for biochar production.[35] However, there is a dearth of information on the synthesis of sulfonated biochar catalyst from eucalyptus tree bark for esterification of fatty acid with methanol to produce FAME (biodiesel).

Thus, this study was aimed to investigate the potentiality of utilizing eucalyptus tree bark as a source of sulfonated biochar-based catalyst for the esterification of oleic acid. The impact of *p*-TSA (sulfonating agent) loading on eucalyptus bark derived-biochar was investigated. Moreover, the impact of esterification process conditions on FAME yield and the recyclability of the spent catalyst were studied in detail.

2. Materials and methods

2.1. Materials

Eucalyptus tree shed barks (ETB) were picked from a dry waste bin at CSIR-Indian Institute of Petroleum, Dehradun, India. *p*-Toluene sulfonic acid monohydrate ($CH_3C_6H_4SO_3H$, ≥98.0%, Merck), oleic acid ($C_{18}H_{34}O_2$, 65–88%, Merck), methanol (CH_3OH, 99.8%), *n*-hexane (99%), methyl heptadecanoate

(99.5%), zinc chloride ($ZnCl_2$, 98%) and hydrochloric acid (HCl, 36%) were all purchased from Sigma-Aldrich Chemical Industries, India.

2.2. Preparation of sulfonated biochar catalyst

The sulfonated ETB biochar catalyst was synthesized *via* a three-step (pyrolysis–activation–sulfonation) process as follows:

2.2.1. Preparation of activated biochar. Firstly, the collected ETB was thoroughly washed with clean water to get rid of sand, dried at 80 °C for 6 h in an oven and then ground into powder using mortar and pestle. After that, the ETB powder was sieved through a 0.3 mm sieve mesh. In order to produce biochar (BC), 50 g of ETB powder was pyrolyzed in a furnace under no oxygen condition at 600 °C and 5 °C min⁻¹ (ramping rate) for 1.5 h. The pyrolyzed material (biochar) was left to cool and kept in a glass container. In order to activate the BC sample, 30 g of eucalyptus biochar was suspended in 200 mL of 3 M $ZnCl_2$ solution, stirred on a magnetic stirrer (at 60 °C for 5 h) and then filtered. The BC residue was thereafter washed several times with deionized water until solution pH attained neutral. Finally, the washed BC sample was dried at 110 °C overnight in an oven and the resulting dark fine powder would henceforth refer to as activated biochar (ABC).

2.2.2. Synthesis of sulfonated biochar catalysts. Herein, the sulfonated biochar catalysts were synthesized *via* the impregnation method. A fixed quantity of the ABC sample of 2 g was suspended in 50 mL of distilled water, and different amounts of *p*-toluene sulfonic acid (*p*-TSA) monohydrate (2, 4, 6 and 8 g) were gently added and stirred on a magnetic stirrer for 5 h at 60 °C. The resulting homogenized solution was then dried at 100 °C for 24 h in an oven. The dried sulfonated biochar catalysts were denoted as *p*-TSA_m/ABC, where *m* stands for the mass ratio of *p*-TSA to activated biochar, *e.g.*, *p*-TSA_2/ABC indicated that 4 g of *p*-TSA was impregnated on 2 g of activated biochar.

2.3. Analysis of sulfonated biochar catalysts

The phases and crystallographic structure, surface functional groups, surface morphology and elemental composition, textural characteristics (specific surface area and pore geometry) and thermal stability of the synthesized *p*-TSA/ABC catalysts were examined by using a powder X-ray diffractometer (D8 Advance, Bruker AXS Gmbh, Germany) with Cukα ($\lambda = 1.5406$ Å) radiation at a scan rate of 0.02° min⁻¹, Fourier transform infrared spectrometer (Perkin Elmer-Spectrum TWO, spectra range: 4000 to 400 cm⁻¹), Micromeritics analyzer (ASAP 2010, USA), field emission-scanning electron microscope (FE-SEM, Quanta 200F, Eindhoven, Netherland) and TGA/DTG instrument (Shimadzu DTG60, Japan; the condition for analysis: N_2 carrier flow rate = 100 mL min⁻¹, heating rate = 15 °C min⁻¹ and temperature range = 30–900 °C), respectively. Moreover, the acid densities of the synthesized sulfonated biochar catalysts were determined using ion-exchange titration procedures reported by Nda-Umar *et al.*[12] For each measurement, 0.05 g of the as-synthesized *p*-TSA/ABC catalyst was suspended in 20 mL of 2 M NaCl solution and stirred for 1 h on a magnetic stirrer. After that, the suspension was filtered, and the filtrate obtained

was titrated against 0.05 M NaOH in the presence of phenolphthalein as an indicator. The acid density (acidity), expressed as mmol NaOH per g cat, was calculated using eqn (1).

$$A_d = \frac{V_{NaOH} \times C_{NaOH}}{M_c} \quad (1)$$

where A_d = acidity (mmol NaOH per g cat), V_{NaOH} = volume of NaOH consumed and M_c = mass of catalyst used.

2.4. Activity test

2.4.1. Esterification of oleic acid. Conversion of oleic acid (OA) to FAME *via* esterification with methanol in the presence of synthesized *p*-TSA/ABC catalyst was carried out in a 100 mL round bottom flask attached with a reflux condenser and a magnetic stirrer. All through the experiments, the flask was immersed in a silicon oil bath to regulate the temperature. For each experiment, a prepared solid acid catalyst (of certain mass) was suspended in methanol, mixed for 10 min, and 10 g of OA was added to the mixture. Thereafter, the reactants and catalyst were heated to the desired reaction temperature and continuous stirring started immediately. In order to avoid mass transfer limitation, the stirring rate was fixed at 500 rpm. Various esterification process parameters, such as temperature (50–80 °C), time (1–5 h), methanol/OA molar ratio (4 : 1–12 : 1) and catalyst loading (1–5 wt%), were evaluated. After the reaction was completed, the product mixture was centrifuged at 7500 rpm for 10 min and the spent catalyst was removed. The centrifuged liquid was then evaporated by rotary evaporator at 80 °C to remove unreacted methanol and water.

2.4.2. Analysis of esterified product. The FAME content in the evaporated product was analyzed by gas chromatography (Agilent GC, 7890A, USA) coupled with flame ionization detector (GC-FID) and capillary column (J & W DH-5HT; dimension: 15 m × 0.32 mm × 0.1 μL) with helium as a carrier gas. For each analysis, 10 μL of the esterified product was dissolved in 200 μL of internal standard (methyl heptadecanoate) and 1 μL of the mixture was thereafter injected into the analyzer for analysis to commence. The oven's initial operating temperature was 60 °C, which was gradually increased to 180 °C at a rate of 15 °C min^{-1}. The temperature was then raised to 230 °C at a rate of 7 °C min^{-1} and held for zero min. Finally, the temperature was set to 350 °C for 10 min at a rate of 30 °C min^{-1}. The FAME yield (Y) was calculated as follows:

$$Y = \frac{(\sum A) - A_I}{A_I} \times \frac{C_I \times V_I}{m} \times 100\% \quad (2)$$

where $\sum A$ indicates overall FAME area from C_{14} to C_{22}, A_I is the peak area associated with the internal standard, V_I and C_I are the volume and concentration of internal standard, respectively, and m is the sample weight. Fig. 1 shows the schematic diagram of the process, which includes sulfonated catalyst preparation and characterization, esterification reaction, catalyst reusability, FAME separation and purification.

2.4.3. Catalyst reusability and stability study. In furtherance of our desire to ascertain the recycling performance of the *p*-TSA/ABC catalyst, we investigated the catalyst stability during reuse. After each experiment, the spent catalyst was collected, washed with *n*-hexane to remove the adsorbed stains and then dried at 100 °C overnight in an oven. Subsequently, the regenerated catalyst was used for another esterification reaction
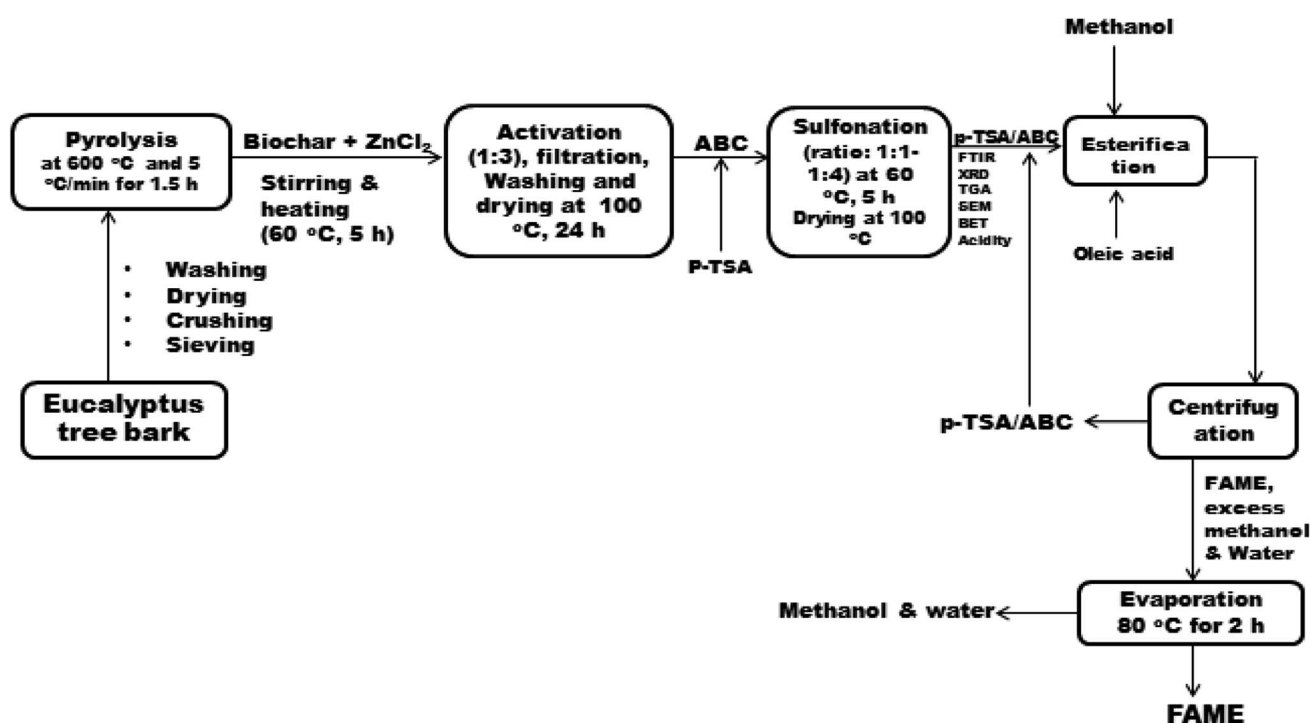

Fig. 1 Schematic representation of the process including catalyst preparation, esterification reaction, catalyst reusability and FAME separation.

under the same experimental conditions. For the leaching test, the sulfonated catalyst was mixed with methanol at 60 °C for 2 h. The methanol was recovered by filtration through a separating funnel and employed for esterification of OA at 65 °C for 2 h and a methanol extract to OA molar ratio of 10 : 1. Moreover, a control experiment in the absence of catalyst was carried out with pure methanol and OA under the same reaction conditions.

3. Results and discussion

3.1. As-synthesized catalyst characterization

In order to gain insight into the properties of the as-synthesized sulfonated biochar catalysts derived from eucalyptus tree bark, FTIR, SEM, EDX, TGA, XRD, N_2 adsorption–desorption isotherm and acidity analyses were carried out and discussed as follows:

3.1.1. FTIR analysis results. The FTIR spectra of the ABC and the *p*-TSA/ABC catalysts at different impregnation ratios are depicted in Fig. 2. The main peaks in the ABC sample occurred at 3539 cm^{-1}, 1629 cm^{-1}, 1144 cm^{-1} and 618 cm^{-1} were attributed to the O–H stretching, NH_2 deformation, C–N stretching and C–O–H twisting, respectively.[36] However, a change in FTIR pattern was observed after impregnating *p*-TSA on activated biochar, with some of the peaks earlier observed on the support material disappeared or shifted. As shown in Fig. 2, all the sulfonated catalysts exhibited a similar FTIR pattern with

Fig. 2 FTIR spectra of (a) ABC and (b–e) sulfonated *p*-TSA/ABC catalysts at different impregnation ratios of *p*-TSA to ABC: (b) 1 : 1, (c) 2 : 1, (d) 3 : 1 and (e) 4 : 1.

numerous peaks, which signified the complexity of the catalysts. The typical absorption bands observed on the spectra of the *p*-TSA/ABC catalysts were N–H stretching vibration at 3457 cm^{-1}, C=O deformation of –COOH at 1648 cm^{-1}, CH_2 deformation at 1498 cm^{-1}, S=O vibration reduction (sulfonic acid bond) at 1356 cm^{-1}, C=S asymmetric stretching at 1209 cm^{-1} and another S=O vibration reduction at 1042 cm^{-1}. It is worthy of mention that appearance of C=S in the spectra suggested that sulfonic (–SO_3H) groups were successfully inserted into the framework in the form of C–SO_3H.[2] These FTIR data obtained were in agreement with the results reported for sulfonated carbon catalyst derived from corncob,[2] coffee residue[1] and palm kernel shells.[12] By comparing the FTIR spectra of ABC and the sulfonated biochar catalysts, it could be concluded that SO_3H groups from the sulfonating agent were present on the catalyst surface, indicating that acid sites were the active centers during the esterification reaction. This is corroborated by the SEM, EDX and XRD analyses.

3.1.2. SEM analysis. Fig. 3 reveals the surface morphologies of ABC and *p*-TSA/ABC catalysts at different impregnation ratios. As evident in Fig. 3a, ABC exhibited a sponge-like, irregular and rough surface morphological structure. Besides, there were numerous pores on its surface. As shown in Fig. 3b–e, however, the pores were blocked due to the impregnation of sulfonating agent on the support material (ABC). It was noticed that the number of pores on the ABC surface reduced as the impregnation ratio increased, indicating that the catalyst surface converged by the SO_3H group from the sulfonating agent. Nevertheless, even upon the sulfonation, the reactants could easily diffuse through the available pores of the sulfonated catalysts and most of the acidic sites were active during the esterification reaction.[29]

3.1.3. EDX analysis. As evident in Table 1, the ABC contained mainly of C followed by O with traces of Zn and Cl due to activating agent ($ZnCl_2$) used for biochar modification, while the *p*-TSA/ABC catalysts had C, O, Si, S, Cl and Zn except for *p*-TSA_4/ABC catalyst without the Cl. It was noticed that the sulfur content increased as loading of *p*-TSA (sulfonating agent) increased, thus confirming successful impregnation of sulfonic acid on the support material (ABC). This result corresponded to the study reported by Zhao *et al.*[29] for biochar-based catalyst from waste pomelo peel. It is important to mention that traces of Si found in *p*-TSA_3/ABC and *p*-TSA_4/ABC could be attributed to presence of impurities in sulfonating agent similar to results reported by Dechakhumwat *et al.* (2019).

3.1.4. TGA analysis. The thermal decomposition trends of the ETB powder, ABC and *p*-TSA_3/ABC are shown in Fig. 4. As seen in Fig. 4a, the ETB exhibited three decomposition stages, with the first weight loss occurred between 30 and 216 °C, which could be due to the water removal. A significant weight loss was noticed in the second stage over the temperature range of 216 °C to 390 °C, which signified simultaneous depolymerization of hemicellulose and degradation of cellulose, usually in the form of gases (NH_3, CO_2 and H_2O).[37,38] Furthermore, TGA curve of ETB was almost constant above 450 °C, which demonstrated the end of the decomposition process. However, it was observed that the decomposition trend of ABC differed
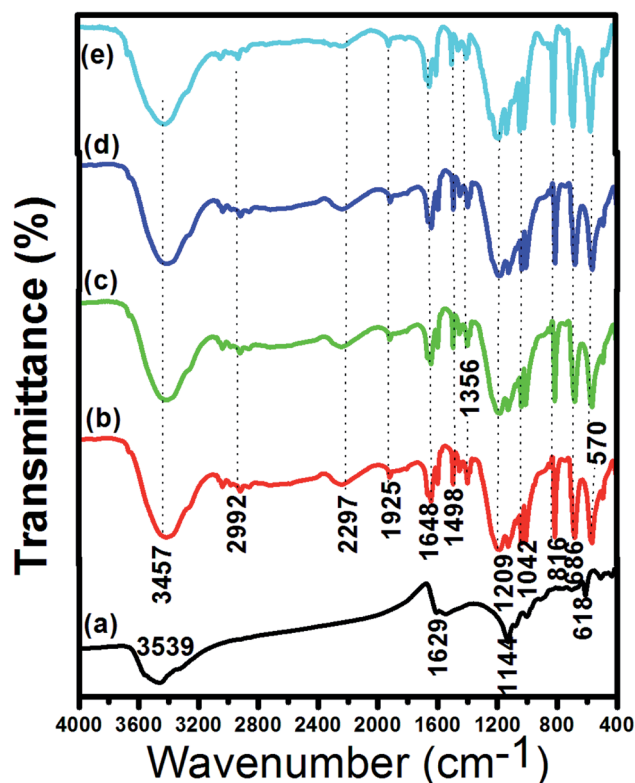
Fig. 3 SEM images of (a) ABC and (b–e) sulfonated *p*-TSA/ABC catalysts at different impregnation ratios of *p*-TSA to ABC: (b) 1 : 1, (c) 2 : 1, (d) 3 : 1 and (e) 4 : 1.
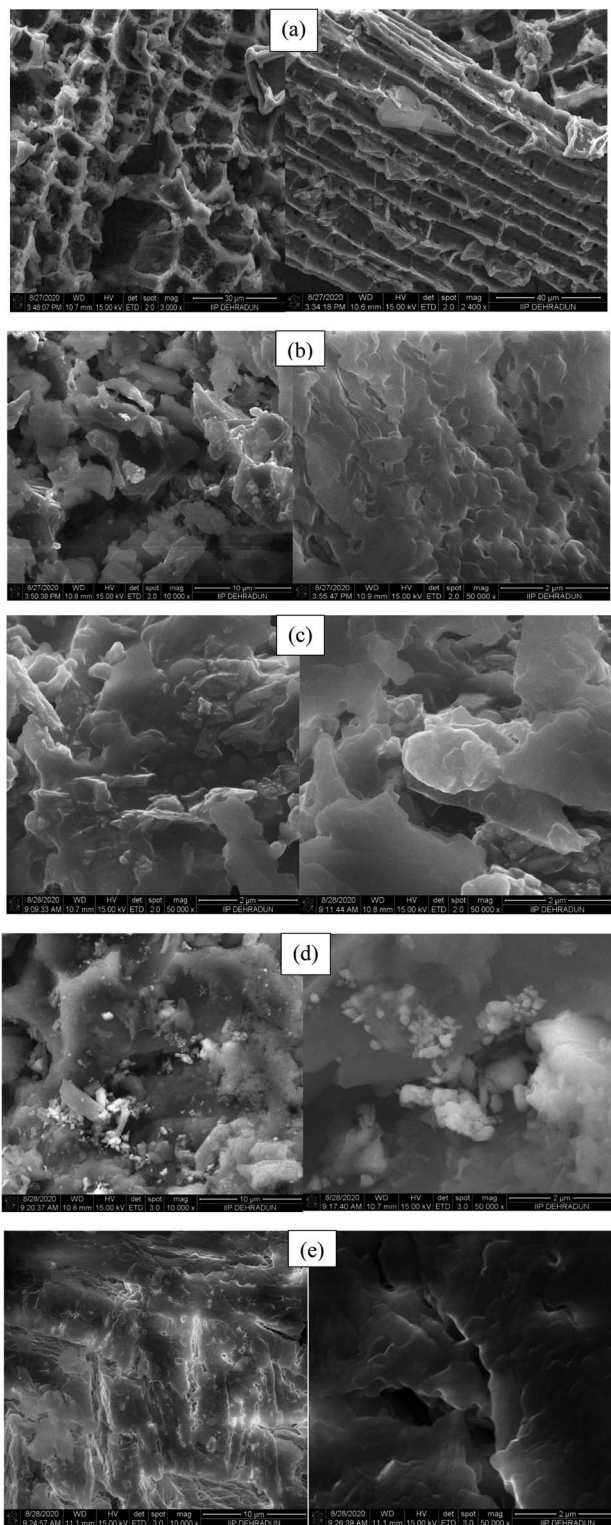
Table 1 EDX analysis for ABC and *p*-TSA/ABC catalysts

Element	Material (wt%)				
	ABC	*p*-TSA$_1$/ABC	*p*-TSA$_2$/ABC	*p*-TSA$_3$/ABC	*p*-TSA$_4$/ABC
C	70.58	42.05	54.01	66.88	64.15
O	27.97	34.20	23.43	20.83	28.98
Cl	0.23	5.14	8.87	1.63	—
Zn	1.23	11.55	8.99	3.44	1.52
Si	—	—	—	0.22	0.09
S	—	5.37	6.08	7.02	7.27

catalyst occurred between 30 and 405 °C, which was ascribed to the simultaneous evaporation of water molecules and degradation of sulfonic acid (–SO$_3$H) groups.[12,21,39] Since degradation of lignin takes place at 200–500 °C,[40,41] the second stage weight loss curve (Fig. 4c), which occurred from 405 to 606 °C, suggested that sulfonation resulted in complete decomposition of lignin as well as complete removal of hemicellulose and cellulose. The TGA data obtained herein was in agreement with the work reported by Dechakhumwat *et al.*[2] However, the last stage of mass loss by the *p*-TSA$_3$/ABC took place above 600 °C, indicating that the sulfonated catalyst was thermally stable due to carbon moiety,[12,42] as corroborated by the FTIR (Fig. 2) and EDX results (Table 1).

3.1.5. XRD analysis. Fig. 5 depicts the XRD patterns of ETB biochar, ABC and *p*-TSA$_3$/ABC catalyst. As seen in the result, the biochar displayed a broad hump peak observed over 2θ angles ranging between the 10–30°, which resulted from the presence of amorphous carbon structure, which was consistent with the (002) plane of the carbon.[2,29] Also, a diffraction peak observed at $2\theta = 35$–50°, broad although depressed and diffused, indicated that the intragraphitic layers were not fully developed.[43] However, the activated biochar sample (Fig. 5b) exhibited some peaks that were attributed to the presence of ZnO phases (34.5°, 36.7° and 56.8°), suggesting the traces of activating agent (ZnCl$_2$) in the studied sample. This observation was in line with
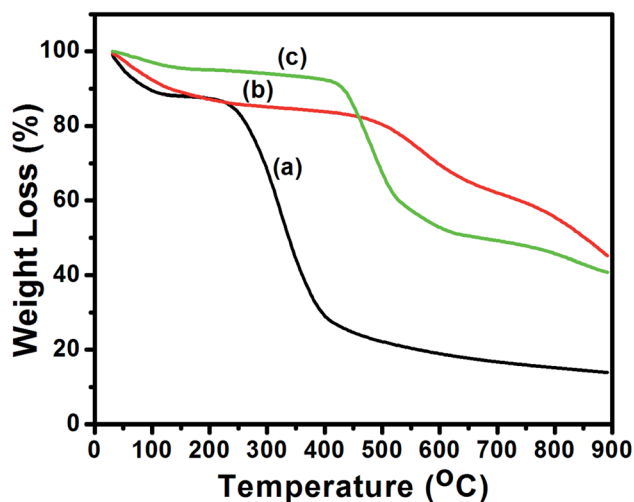
from that of ETB probably due to pyrolysis and activation effects. The ABC exhibited two stages of weight loss (Fig. 4b), while *p*-TSA$_3$/ABC catalyst displayed three major decomposition stages, as seen in Fig. 4c. The first stage of decomposition of the

Fig. 4 TGA results for (a) ETB, (b) ABC and (c) *p*-TSA$_3$/ABC catalyst.
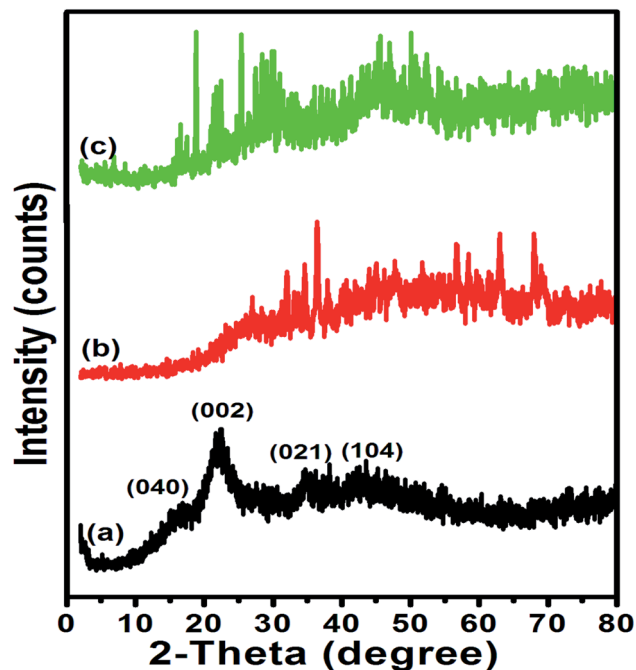
Fig. 5 XRD pattern of (a) ETB biochar (b) ABC and (c) p-TSA$_3$/BC catalyst.

Fig. 6 N$_2$ adsorption−desorption isotherms of ABC and p-TSA$_3$/ABC catalyst.

Table 2 Textural characteristics of activated biochar and sulfonated biochar catalyst

	Sample	
Parameter	ABC	p-TSA$_3$/ABC catalyst
BET surface area (m^2 g^{-1})	217	31
Total pore volume (cm^3 g^{-1})	0.21	0.24
Average pore diameter (nm)	49.9	24.6

results reported by Ngaosuwan *et al.*,[1] who modified coffee residue biochar with ZnCl$_2$, whereby ZnO phases were detected in the diffractogram of the activated carbon.

Meanwhile, there was visible change in the XRD pattern after sulfonation of activated biochar as seen in Fig. 5c. By comparing the diffractograms of ETB biochar and synthesized sulfonated biochar catalyst, there was reappearance of peak (at around 2θ = 26.7°), corresponding to the (002) plane of amorphous carbon. It is worthy of note that the presence of amorphous carbon in the sulfonated eucalyptus bark biochar catalyst agreed reasonably well with the XRD data reported on sulfonated carbon catalysts obtained from glucose,[14] corncob,[2] waste pomelo peel[29] and pam kernel shell.[12] Besides, the results were corroborated by the TGA and EDX analyses.

3.1.6. Textural characteristics analysis. Fig. 6 shows the N$_2$ sorption isotherms of ABC and p-TSA$_3$/ABC. It was clear that the sulfonated eucalyptus biochar catalyst manifested a feature corresponding to the mesoporous material (stage IV isotherm). In addition, the synthesized catalyst exhibited a hysteresis loop corresponding to H3, which suggested that it was aggregates of plate-like particles forming slit-like pores.[44] However, the activated biochar exhibited type II isotherm, which was a feature of macroporous material. As seen in Table 2, the specific surface area of the ABC sample exceeded that of the sulfonated catalyst, in conformity with the less porous structure observed in the results of SEM analysis. The sulfonation resulted in partial blockage of some pores by the sulfonating agent (p-TSA) impregnated on the ABC (support material). Nevertheless, going by the preliminary results (see Fig. 7), the partial blockage of the p-TSA$_3$/ABC catalyst had nothing to do with the catalyst performance, as also reported by Zhao *et al.*[29]
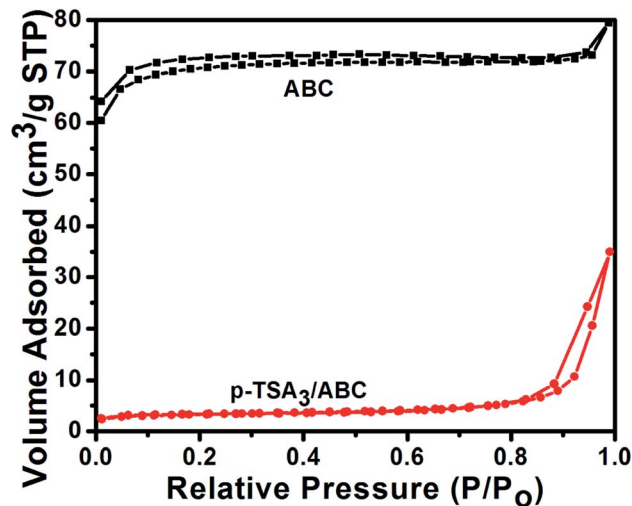
3.2. Influence of sulfonating agent loading on activated biochar

The synthesized catalyst samples (ABC, p-TSA$_1$/ABC, p-TSA$_2$/ABC, p-TSA$_3$/ABC and p-TSA$_4$/ABC denoted by the letters A to E, respectively) were tested in order to gain insight into their
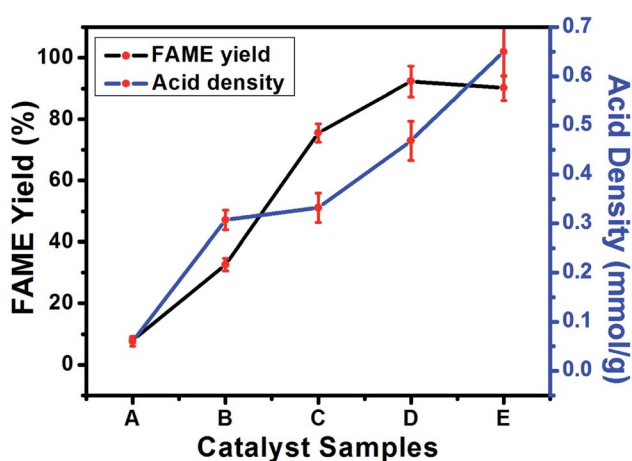

Fig. 7 FAME yield and acid density against various catalysts used (Catalyst loading = 1.5 wt%, methanol/OA molar ratio = 12 : 1, temperature = 60 °C and reaction time = 3 h).

catalytic performance in the esterification process, and the results are depicted in Fig. 7. As seen in the result, the activated biochar appeared to be ineffective for esterification of OA due to the insufficient acidic site on its surface, thereby inhibiting the reaction from moving towards equilibrium. However, after impregnation of sulfonic acid on ABC, a significant increase in FAME yield was recorded with an increase in the amount of sulfonating agent used for impregnation. The trend displayed in Fig. 7 revealed an increase in the yield of FAME from $30.11 \pm 0.71\%$ to $92.33 \pm 2.01\%$, with a corresponding increase in the impregnation ratio from 1 : 1 to 3 : 1, respectively. There was a decrease in FAME yield when the impregnation ratio increased to 4 : 1. The presumed reason for this observation was that p-TSA was well dispersed on the ABC surface at low concentration of the sulfonating agent, but at higher concentration of p-TSA the sulfonic acid molecules deposited on the support material surface and blocked the active sites.[1,13] These results indicated that p-TSA$_3$/ABC is the best among the synthesized sulfonated catalysts. The astounding performance of the catalyst could be attributed to the impregnation effect, which resulted in the even distribution of SO$_3$H (sulfonic acid group) on the ABC surface that improved the acidity of the sulfonated catalyst, thus enhancing its catalytic performance.

Also, Fig. 7 showed that the acid density of the synthesized sulfonated catalyst increased as the concentration of the sulfonating agent increased. The values of acid density obtained from acid–base titration ranged from 0.06–0.65 mmol g^{-1} with

p-TSA$_4$/ABC catalyst exhibited the highest acidity. As expected, a further increase in the impregnation ratio would enhance total acidity but did not guarantee high FAME yield because the porosity of the catalyst played a pivotal role in FAME conversion.[45] This result was similar to the work reported by Dechakhumwat $et\ al.$[2]

3.3. Influence of esterification process conditions on FAME yield

Fig. 8a shows the influence of catalyst loading on the esterification of oleic acid using p-TSA$_3$/ABC catalyst. The catalyst amount was varied from 1 to 5 wt%. From the result, it was observed that the FAME yield increased with the amount of catalyst up to 4.0 wt% and thereafter decreased as the catalyst dosage increased to 5.0 wt%. The reason for this observation was that high catalyst concentration raised the viscosity of the reaction mixture, which inhibited the diffusion of reactant molecules to the catalyst active centers, thereby leading to saturation and mass transfer limitation during the reaction process.[46] This result indicated that increasing the catalyst dosage does not guarantee FAME yield increase but increases the overall biodiesel production cost. Since 4.0 wt% catalyst loading gave the maximum FAME yield, it was selected as the optimum value and used for the subsequent esterification studies.
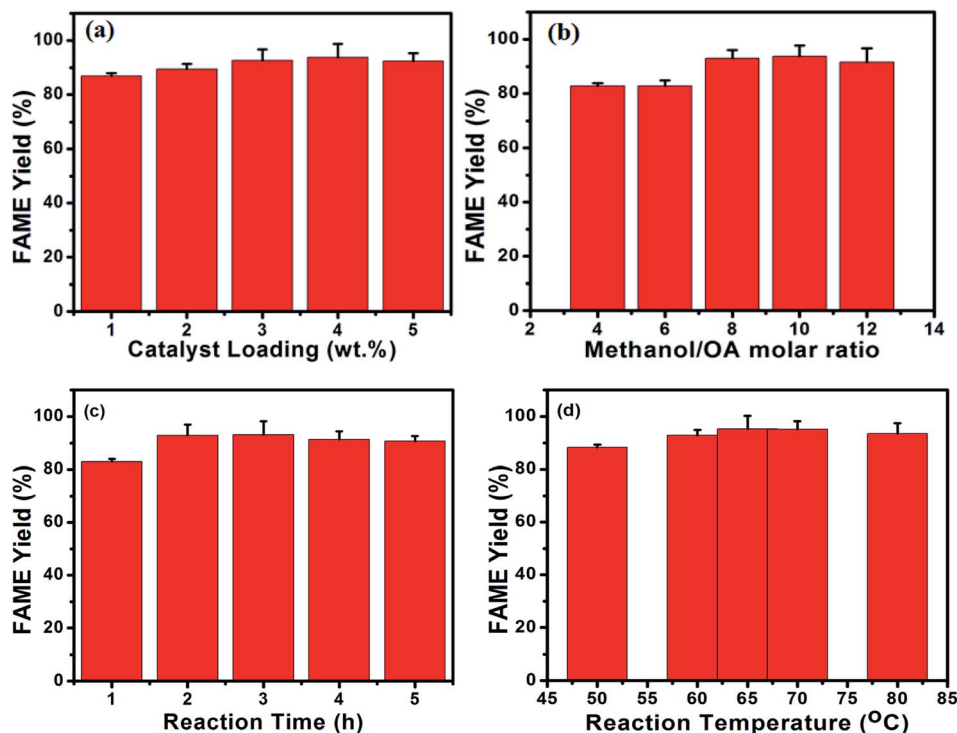

Fig. 8 (a) Esterification reaction using p-TSA$_3$/ABC catalyst at different catalyst loadings and FAME yield at fixed time = 3 h, methanol/OA molar ratio = 8 : 1 and temperature = 65 °C, (b) yield of FAME at different methanol/OA molar ratios at fixed reaction time = 3 h, temperature = 65 °C and catalyst loading = 4.0 wt%, (c) influence of reaction time on FAME yield at constant temperature = 65 °C, catalyst loading = 4.0 wt% and methanol/OA molar ratio = 10 : 1 (d) FAME yield at various temperatures, reaction time = 2 h, catalyst loading = 4.0 wt% and methanol/OA molar ratio = 10 : 1.

The effect of alcohol to OA molar ratio on FAME yield was also investigated, and the result is shown in Fig. 8b. As seen from the result, the maximum FAME yield was obtained when methanol/OA molar ratio of 10 : 1 was used because the volume of methanol used was enough to shift the esterification process forward to attain high FAME yield. However, there was a slight decrease in FAME yield when the molar ratio of methanol to OA was 12 : 1 because a large volume of methanol inhibited the separation of methyl esters and water phases, thus decreasing the yield of the final product.[29,47] Therefore, the optimum methanol/OA molar ratio of 10 : 1 was selected and employed for further investigations.

As seen in Fig. 8c, the FAME yield increased from 82.9% to 93.18% when reaction time increased from 1 to 3 h. However, as the reaction duration exceeded 3 h, no increase in FAME yield was noticed. Since the esterification process was a reversible reaction, increasing the reaction duration could drive the reaction backward and deactivate the catalyst, which reduced the FAME yield.[29] In spite of the fact that maximum FAME yield was obtained at 3 h, the reaction time of 2 h was selected as optimum value because only a little increase in the FAME yield (0.26%) was noticed with a 1 h difference in duration. It is economical and facile to carry out the reaction process at a low reaction time as less energy would be required.[46]

In order to investigate the influence of reaction temperature on FAME yield, the esterification experiments were carried out with temperature varying from 50 to 80 °C while keeping other variables constant. As seen in Fig. 8d, FAME yield increased with increasing temperature up to 65 °C and then decreased as the temperature rose above the optimum value. This observation was due to methanol vaporizing as the reaction temperature exceeded its boiling point (around 65 °C), resulting in low biodiesel yield. Thus, 65 °C was chosen as the optimum temperature.

3.4. Reusability study of p-TSA$_3$/ABC catalyst

Herein, the stability of the p-TSA$_3$/ABC catalyst was studied by subjecting the spent catalyst to successive reaction runs under the established optimum operational parameters. As shown in Fig. 9, the yield of FAME gradually decreased from 80.32% to 35.78% due to a significant reduction in the number of active sites caused by catalyst surface poisoning by FFA molecules, which reduced the FAME yield.[1,46,48] Leaching analysis conducted under optimum conditions revealed that 11.45% of OA was converted when the used methanol reacted with the organic acid. On the other hand, esterification of OA with pure methanol in the absence of catalyst resulted in a low OA conversion (1.08%). These findings indicated that leaching of the P-TSA$_3$/ABC catalyst occurred. The reduction in the FAME yield for several runs during esterification reaction was attributed to the catalyst leaching. The observed trend agreed with the results reported by Fraile et $al.$[49] who concluded that the sulfonated carbon catalyst with high SO$_3$H acid site density leached due to the weak interaction between poly-aromatic hydrocarbon structure and SO$_3$H species.

3.5. Characterization of spent p-TSA$_3$/ABC catalyst

The microstructure analysis of the reused p-TSA$_3$/ABC catalyst had been carried out after five successive runs, and the SEM
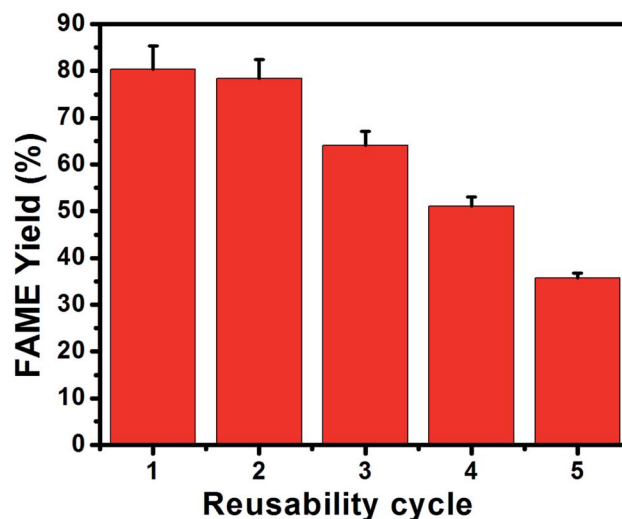

Fig. 9 Reusability study of p-TSA$_3$/ABC catalyst under optimum reaction conditions (catalyst loading = 4.0 wt%, temperature = 65 °C, reaction time = 2 h and methanol/OA molar ratio = 10 : 1).

results are shown in Fig. 10. By comparing the SEM micrographs of the fresh and spent p-TSA$_3$/ABC catalysts, it appeared that there was a change in the morphological structure of the fresh catalyst after it was reused as the spent catalyst displayed (Fig. 10b) an irregular structure with agglomerated particle, attributed to the blockage of some pores by high molecular weight fatty acid which reduced the number of the catalyst active sites. This suggested the reason why the FAME yield reduced as the reusability cycle increased. This was in good agreement with the functional groups observed in the FTIR spectra of the recovered catalysts after the first and last (fifth) cycles (see Fig. 11).
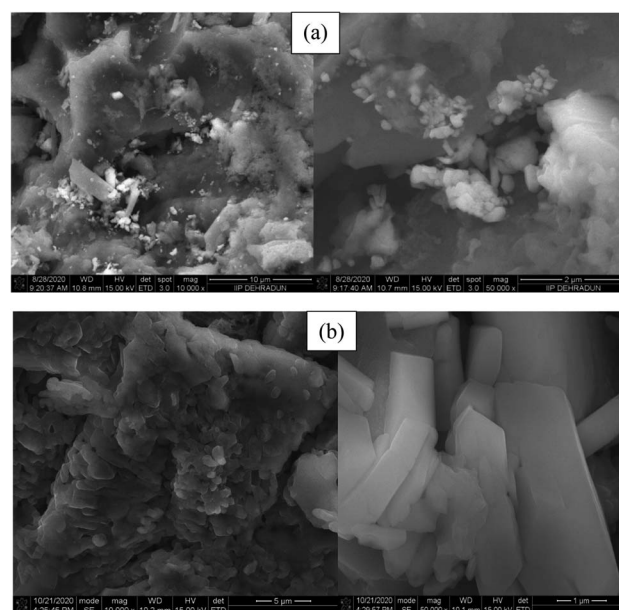

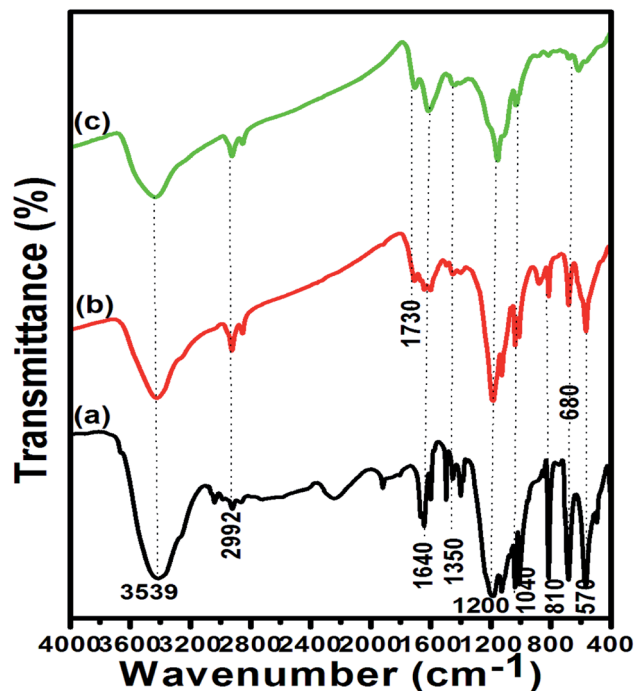Fig. 10 SEM images of (a) fresh and (b) spent p-TSA$_3$/ABC catalysts.

Fig. 11 FTIR spectra of (a) fresh p-TSA$_3$/ABC (b) reused p-TSA$_3$/ABC for the first time and (c) reused p-TSA$_3$/ABC for the last time.

Table 3 EDX analysis for fresh p-TSA$_3$/ABC and spent p-TSA$_3$/ABC used for last cycle

	Material (wt%)	
Element	Fresh p-TSA$_3$/ABC	Spent p-TSA$_3$/ABC
C	66.88	40.62
O	20.83	44.00
Cl	1.63	—
Zn	3.44	6.18
Si	0.22	—
S	7.02	2.12

As seen in the FTIR result (Fig. 11), the peak associated with C=O (ester) stretching at 1730 cm^{-1} was observed on the spectra of the reused catalysts. Also, it appeared that the intensity of the peak at 2992 cm^{-1} (C–H stretching vibration of methyl group) increased after first and last time reuse, which confirmed the poisoning of catalyst surface sites by methyl esters.[50] Furthermore, the intensity of those peaks (1200 cm^{-1} and 1040 cm^{-1}) that were associated with the SO$_3$H functional group decreased as seen on the spectrum of the spent catalyst used for the last cycle, which might be attributed to the loss of acidic sites, as confirmed by EDX results (Table 3) which showed that, the spent p-TSA$_3$/ABC catalyst contained lower sulfur composition compared to the fresh catalyst, thus suggesting the leaching of catalyst active ingredient. Also, the increase in oxygen content of the spent catalyst after regeneration suggested that its treatment with hexane favoured the formation of oxygenated groups as corroborated by the FTIR results. This result complied with the findings reported by Zhao et al.,[29] who produced biodiesel from high free fatty acid feedstock using biochar-based acid catalyst from waste pomelo peel.

3.6. Comparison of the p-TSA$_3$/ABC with previously reported catalysts

Table 4 compares catalytic performance between the p-TSA$_3$/ABC and previously reported biomass-derived solid acid catalysts in the esterification reaction. As seen in the listed data, it was evident that the prepared p-TSA$_3$/ABC catalyst exhibited excellent catalytic activity compared to other biomass-based catalysts, suggesting that the eucalyptus-derived solid acid catalyst was effective in converting oleic acid to biodiesel via esterification reaction and was a potential candidate for industrial use.

3.7. Physicochemical characteristics of biodiesel obtained from oleic acid

Any fuel/biofuel whose properties meet the EN 14214 and ASTM D6757 standards can power a diesel engine. The properties of the biodiesel sample produced through the esterification of oleic acid over p-TSA$_3$/ABC catalyst are contained in Table 5. As

Table 4 Comparison of the catalytic activity of various biomass derived-carbon catalysts in esterification reaction[a]

Catalyst	Support source	Feedstock	Experimental reaction parameters				FAME yield (%)	Reference
			C (wt%)	t (h)	T (°C)	M		
TsOH/biochar	Corncob	Oleic acid	69.0	8.0	60	15 : 1	>80	2
H$_2$SO$_4$/biochar	Corncob	Oleic acid	69.0	8.0	60		>80	2
SCAC	Coffee residue	Caprylic acid	5.0	4.0	60	3 : 1	71.5	1
H$_2$SO$_4$/rice husk char	Rice husk	Oleic acid	5.0	2.0	110	4 : 1	98.7	18
H$_2$SO$_4$/Magnetic biochar	Palm empty fruit bunches	Oleic acid	5.0	1.5	150	8 : 1	97.6	51
H$_2$SO$_4$/Coconut shell biochar	Coconut shell	Palm fatty acid distillate	7.0	4.0	60	12 : 1	82.9	52
H$_2$SO$_4$/biochar	Murumuru kernel shell	Oleic acid	5.0	1.5	90	10 : 1	97.2	53
p-TSA$_3$/ABC	ETSB	Oleic acid	4.0	2	65	10 : 1	97.05 ± 0.28	This study

^{a} C = catalyst loading, t = time, T = temperature, M = methanol/OA molar ratio, SCAC = sulfonated activated carbon catalyst, TsOH = p-toluenesulfonic acid.

Table 5 Physicochemical and fuel properties of biodiesel obtained from esterification of oleic acid using *p*-TSA$_3$/ABC catalyst

Property	Oleic acid based biodiesel	ASTM specification	ASTM test
Density (g cm^{-3})	0.8863	—	D4052
Kinematic viscosity (mm^2 s^{-1})@40 °C	4.82	1.9–6.0	D445
Acid value (mg KOH g^{-1})	1.32	≤0.8	—
Flash point (°C)	158	≥130	D-93
Pour point (°C)	−3	−15 to 10	—
Cloud point (°C)	+7	−3 to 12	D2500
Specific gravity@20 °C	0.8869	0.86–0.90	D4052
API gravity, API	31.0	—	—

shown in the list, all the fuel characteristics of the synthesized biodiesel were found to be in agreement with the ASTM values except acid value that exceeded the limit.

4. Conclusions

Synthesized sulfonated biochar catalyst derived from eucalyptus tree bark exhibited amorphous carbon structure with high acidity and numerous functional groups. The maximum (Fig. 1) FAME yield (>96%) was obtained over the *p*-TSA$_3$/ABC catalyst, where the dominance of the SO$_3$H acid site was perceived. At 65 °C for 2 h with 10 : 1 methanol/OA molar ratio and 4.0 wt% catalyst loading, a maximum FAME content of 97.05 ± 0.28% was obtained. Additionally, the reusability study showed that the solid acid catalyst was relatively stable when subjected to successive runs. Thus eucalyptus tree bark could be a starting material for a solid acid catalyst for biodiesel production.

Conflicts of interest

The authors declare that they have no known competing financial interests or personal relationships that could have appeared to influence the work reported in this paper.

Acknowledgements

References

1 K. Ngaosuwan, J. G. Goodmin Jr and P. Prasertdham, A green sulfonated carbon-based catalyst derived from coffee residue for esterification, *Renew. Energ.*, 2016, **86**, 262–269, DOI: 10.1016/j.renene.2015.08.010.

2 S. Dechakhumwat, P. Hongmanorom, C. Thunyaratchotanon, S. M. Smith, S. Boonyuen and A. Luengnaruemitchai, Catalytic activity of heterogeneous acid catalysts derived from corncob in the esterification of oleic acid with methanol, *Renew. Energ.*, 2020, **148**, 897–906, DOI: 10.1016/j.renene.2019.10.174.

3 E. Lotero, Y. Liu, D. E. Lopez, K. Suwannakarn, D. A. Bruce and J. G. Goodwin Jr, Synthesis of biodiesel via acid catalysis, *Ind. Eng. Chem. Res.*, 2005, **44**, 5353–5363, DOI: 10.1021/ie049157g.

4 H. L. Tran, Y. J. Ryu, D. H. Seong, S. M. Lim and C. G. Lee, An effective acid catalyst for bioidiesel production from impure raw feedstocks, *Biotechnol. Bioprocess. Eng.*, 2013, **18**, 242–247, DOI: 10.1007/s12257-012-0674-1.

5 M. Di Serio, R. Tesser, M. Dimiccoli, F. Cammarota, M. Nastasi and E. Santacesaria, Synthesis of biodiesel via homogeneous Lewis acid catalyst, *J. Mol. Catal. A: Chem.*, 2005, **239**, 111–115, DOI: 10.1016/j.molcata.2005.05.041.

6 X. Tang and S. Niu, Preparation of carbon-based solid acid with large surface area to catalyze esterification for biodiesel production, *J. Ind. Eng. Chem.*, 2019, **69**, 187–195, DOI: 10.1016/j.jiec.2018.09.016.

7 T. T. Liu, Z. L. Li, W. Li, C. J. Shi and Y. Wang, Preparation and characterization of biomass carbon-based solid acid catalyst for the esterification of oleic acid with methanol, *Bioresour. Technol.*, 2013, **4**, 56–64, DOI: 10.1016/j.biortech.2013.01.163.

8 Y. C. Sharma, B. Singh and J. Korstad, Application of an efficient non-conventional heterogeneous catalyst for biodiesel synthesis form pongamia pinnata oil, *Energy Fuels*, 2010, **24**, 3223–3231, DOI: 10.1021/ef901514a.

9 F. A. Dawodu, O. Ayodele, J. Xin, S. Zhang and D. Yan, Effective conversion of non-edible oil with high free fatty acid into biodiesel by sulfonated carbon catalyst, *Appl. Energy*, 2014, **62**, 819–826, DOI: 10.1016/j.apenergy.2013.10.004.

10 W. Y. Lou, Q. Guo, W. J. Chen, M. H. Zong, H. Wu and T. J. Smith, A highly active bagasse derived solid acid catalyst with properties suitable for production of biodiesel, *ChemSusChem*, 2012, **5**, 1533–1541, DOI: 10.1002/cssc.201100811.

11 A. Mallick, M. Mukhopadhyyay and S. Ash, Synthesis, characterization and performance evaluation of a solid acid catalyst prepared from coconut shell for hydrolyzing pretreated *Acacia nilotica* heartwood, *J. Inst. Eng. (India): Ser. B*, 2020, **101**, 69–76, DOI: 10.1007/s40034-019-00153-1.

12 U. I. Nda-Umar, I. Ramli, E. N. Muhamad and Y. H. Taufiq-Yap, *Synthesis and characterization of sulfonated carbon catalysts derived from biomass waste and its evaluation in glycerol acetylation*, Biomass Conversion and Biorefinery, 2020, DOI: DOI: 10.1007/s13399-020-00784-0.

13 R. Aafaqi, A. R. Mohamed and S. Bhatia, Kinetics of esterification of palmitic acid with isopropanol using p-toluene sulfonic acid and zinc ethanoate over silica gel as catalysts, *J. Chem. Technol. Biotechnol.*, 2004, **79**, 1127–1134, DOI: 10.1002/jctb.1102.

14 B. Zhang, J. Ren, X. Liu, Y. Guo, L. Guenzhong and Y. Wang, Novel sulfonated carbonaceous materials from p-toluenesulfonic acid/glucose as a high performance solid-acid catalyst, *Catalyst Communication*, 2010, **111**, 629–632, DOI: 10.1016/j.catcom.2010.01.010.

15 F. L. Pua, Z. Fang, S. Zakaria, F. Guo and C. H. Chia, Direct production of biodiesel from high acid value *Jatropha* oil with solid acid catalyst derived from lignin, *Biotechnology and Biofuel*, 2011, **4**, 56–64, DOI: 10.1186/1754-6834-4-56.

16 P. A. Russo, M. M. Antunes, P. Neves, P. V. Wiper, E. Fazio, F. Neri, F. Barreca, L. Marfa, M. Fillinger, N. Pinna and A. A. Valente, Solid acids with SO_3H groups and tunable surface properties versatile catalysts for biomass conversion, *J. Mater. Chem. A*, 2014, **30**, 11813–11824, DOI: 10.1039/C4TA02320J.

17 H. Y. Chen and Z. W. Cui, A Microwave-sensitive solid acid catalyst prepared from sweet potato via a simple method, *Catalyst*, 2016, **6**, 211, DOI: 10.3390/catal6120211.

18 M. Li, D. Chen and X. Zhu, Preparation of solid acid catalyst from rice husk char and its catalytic performance in esterification, *Chin. J. Catal.*, 2013, **34**, 1674–1682, DOI: 10.1016/S1872-2067(12)60634-2.

19 W. A. Carvalho, T. S. Galhardo and M. Simone, Preparation of sulfonated carbon from rice husk and their application in catalytic conversion of glycerol, *ACS Sustainability and Chemical Engineering*, 2013, **1**, 1381–1389, DOI: 10.1021/sc400117t.

20 A. R. Lathiya, D. V. Bhatt and K. C. Maheria, Synthesis of sulfonated carbon catalyst from waste orange peel for cost effective biodiesel production, *Bioresour. Technol. Rep.*, 2018, **2**, 69–76, DOI: 10.1016/j.biteb.2018.04.007.

21 I. Thushari and S. Babel, Sustainable utilization of waste palm oil and sulfonated carbon catalyst derived from coconut meal residue for biodiesel production, *Bioresour. Technol.*, 2020, **248**, 199–203, DOI: 10.1016/j.biortech.2017.06.106.

22 J. Laonapornchaiphan, C. B. Smith and S. M. Smith, One-step preparation of carbon-based solid acid catalyst from water hyacinth leaves for esterification of oleic acid and dehydration of xylose, *Chem. – Asian J.*, 2017, **12**, 3178–3186, DOI: 10.1002/asia.201701369.

23 G. M. A. Bureros, A. A. Tanjay, D. E. S. Cuizon, A. W. Go, L. K. Cabatingan, R. C. Agapay and Y. H. Ju, Cacao shell-derived solid acid catalyst for esterification of oleic acid with methanol, *Renew. Energ.*, 2019, **138**, 489–501, DOI: 10.1016/j.renene.2019.01.082.

24 M. L. Tao, H. Y. Guan, X. H. Wang, Y. C. Liu and R. F. Louh, Fabrication of sulfonated carbon catalyst from biomass waste and its use for glycerol esterification, *Fuel Process. Technol.*, 2015, **138**, 355–360, DOI: 10.1016/j.fuproc.2015.06.021.

25 S. Singh, M. A. Nahil, X. Sun, C. Wu, J. Chen, R. Shen and P. T. Williams, Novel application of cotton stalk as a waste derived catalyst in the low temperature SCR-deNO$_x$ process, *Fuel*, 2013, **105**, 585–594, DOI: 10.1016/j.fuel.2012.09.010.

26 E. Sabio, A. Murillo, S. Roman and B. Ledesma, Conversion of tomato-peel waste into solid fuel by hydrothermal carbonization: Influence of the processing variables, *Waste Manage.*, 2016, **47**, 122–132, DOI: 10.1016/j.wasman.2015.04.016.

27 D. Licursi, C. Antonettic, S. Fulignati, S. Vitolo, M. Puccini, E. Ribechini, L. Rernazzani and A. M. R. Galletti, In-depth characterization of valuable char obtained from hydrothermal Conversion of hazelnut shells to levulinic acid, *Bioresour. Technol.*, 2017, **244**, 880–888, DOI: 10.1016/j.biortech.2017.08.012.

28 I. M. Ogbu, V. I. E. Ajiwe and C. P. Okoli, Performance evaluation of carbon-based heterogeneous acid catalyst derived from hura crepitans seed pod for esterification of high FFA vegetable oil, *Journal of Bioengineering Resources*, 2018, **11**, 772–783.

29 C. Zhao, P. Lv, L. Yang, S. Xing, W. Luo and Z. Wang, Biodiesel synthesis over biochar-based catalyst from biomass waste pomelo peel, *J. Environ. Manage.*, 2018, **160**, 477–485, DOI: 10.1016/j.enconman.2018.01.059.

30 F. Ezebor, M. Khairuddeen, A. Z. Abdullah and P. L. Boey, Oil palm trunk and sugarcane baggase derived solid acid catalysts for rapid esterification of fatty acids and moisture-assisted transesterification of oils under pseudo-infinite methanol, *Bioresour. Technol.*, 2014, **157**, 254–262, DOI: 10.1016/j.biortech.2014.01.110.

31 J. W. Gabhane, V. P. Bhange, P. D. Patil, S. T. Bankar and S. Kumar, Recent trends in biochar production methods and its application as a soil health conditioner: a review, *SN Appl. Sci.*, 2020, **2**, 1307, DOI: 10.1007/s42452-020-3121-5.

32 L. Liu, L. Yang and S. Fan, Preparation of KOH and H_3PO_4 modified biochar and its application in methylene blue removal aqueous solution, *Processes*, 2019, **7**, 891, DOI: 10.3390/pr7120891.

33 L. Khenniche and F. Aissani, Preparation and characterization of carbons from coffee residue: adsorption of salicylic acid on the prepared carbons, *J. Chem. Eng. Data*, 2010, **55**, 728–734, DOI: 10.1021/je900426a.

34 S. Martini, S. Afroze and K. A. Roni, Modified eucalyptus bark as a sorbent for simultaneous removal of COD, oil and Cr(III) from industrial wastewater, *Alexandria Eng. J.*, 2020, **59**, 1637–1648.

35 R. M. D. Kanouo, S. E. Allaire and A. D. Munson, Quantity of biochars made from eucalyptus tree bark and corncob using a pilot-scale retort kiln, *Waste Biomass Valorization*, 2018, **9**, 899–909, DOI: 10.1007/s12649-017-9884-2.

36 B. H. Hameed, R. R. Krishni and S. A. Sata, A novel agricultural waste adsorbent for the removal of cationic dye from aqueous solution, *J. Hazard. Mater.*, 2009, **162**, 305–311, DOI: 10.1016/j.jhazmat.2008.05.036.

37 A. Luenenaruemitchai and C. Anupapwisetkul, Surface morphology and cellulose structure of *Nupier* grass pretreated with the ionic liquid 1-ethyl-3-methyllimidazolium acetate combined with either water or dimethyl sulfoxide as a co-solvent under microwave irradiation, *Biomass Convers. Biorefin.*, 2020, **10**, 435–446, DOI: 10.1007/s13399-019-00422-4.

38 E. M. Santos, A. P. D. C. Teixeira and F. G. Da Silva, New heterogeneous catalyst for the esterification of fatty acid produced by surface aromatization/sulfonation of oil seed cake, *Fuel*, 2015, **150**, 408–414, DOI: 10.1016/j.fuel.2015.02.027.

39 N. Nagasumdaram, M. Kokila, P. Santhosh and A. Lalitha, SO_3H@carbon powder derived from waste orange peel: an efficient, nano-sized greener catalyst for the synthesis of dihydropyranol [2,3-c] pyrazole derivatives, *Adv. Powder Technol.*, 2020, **31**, 1516–1528, DOI: 10.1016/j.apt.2020.01.012.

40 M. Brebu and C. Vasile, Thermal degradation of lignin- A review, *Cellulose Chemical Technology*, 2010, **44**, 353–363.

41 S. Shankar, J. P. Reddy and J. M. Rhim, Effect of lignin on water vapour barrier, mechanical and structural properties of agar/lignin composite films, *Int. J. Biol. Macromol.*, 2015, **81**, 267–273, DOI: 10.1016/j.ijbiomac.2015.08.015.

42 J. L. Figueiredo, Fucntionalization of porous carbons for catalytic applications, *J. Mater. Chem. A*, 2013, **1**, 9351, DOI: 10.1039/C3TA10876G.

43 B. S. Girgis, Y. M. Temerk, M. M. Gadelrab and I. D. Abdullah, X-ray diffraction patterns of activated carbons prepared under various conditions, *Carbon Sci.*, 2007, **8**(2), 95–100, DOI: 10.5714/CL.2007.8.2.095.

44 H. Bel Hadjtaief, M. E. Gahvez, M. B. Zina and P. Dacosta, TiO_2/clay as a heterogeneous catalyst in photocatalytic/photochemical oxidation of anionic reactive blue 19, *Arabian J. Chem.*, 2019, **12**, 1454–1462, DOI: 10.1016/j.arabjc.2014.11.006.

45 A. Aldana-Perez, L. Lartundo-Rojas, R. Gomez and M. E. Nino-Gomez, Sulfonic groups anchored on mesoporous carbon starbon s-300 and its use for the esterification of oleic acid, *Fuel*, 2012, **100**, 128–139, DOI: 10.1016/j.fuel.2012.02.025.

46 M. A. Olutoye, S. W. Wong, L. H. Chin, S. W. Amani, M. Asif and B. H. Hameed, Synthesis of fatty acid methyl esters via the transesterification of waste cooking oil by methanol with a barium-modified montmorillonite K10 catalyst, *Renew. Energ.*, 2016, **86**, 392–398, DOI: 10.1016/j.renene.2015.08.016.

47 Y. H. Tan, M. O. Abdullah, C. Nolasco-Hipolito and Y. H. Taufiq-Yap, Waste ostrich- and chicken-eggshells as heterogeneous base catalyst for biodiesel production from used cooking oil: Catalyst characterization and biodiesel yield performance, *Appl. Energy*, 2015, **160**, 58–70, DOI: 10.1016/j.apenergy.2015.09.023.

48 A. S. Yusuff, A. K. Bhonsle, D. P. Bangwal and N. Atray, Development of a barium-modified zeolite catalyst for biodiesel production from waste frying oil: Process optimization by design of experiment, *Renew. Energ.*, 2021, **177**, 1253–1264, DOI: 10.1016/j.renene.2021.06.039.

49 J. M. Fraile, E. Garcia-Bordeje, E. Pires and L. Roldan, New insights into the strength and accessibility of acid sites of sulfonated hydrothermal carbon, *Carbon*, 2014, **77**, 1157–1167.

50 A. S. Yusuff, M. Kumar, B. O. Obe and N. Atray, Calcium oxide supported on coal fly ash (CaO/CFA) as an efficient catalyst for biodiesel production from *Jatropha curcas* oil, *Top. Catal.*, 2021, DOI: 10.1007/s11244-021-01478.

51 A. S. N. Jenie, A. Kristieni, S. Deni, S. Khaerudins and K. Takeishi, Sulfonated magnetic nanobiochar as heterogeneous acid catalyst for esterification reaction, *J. Environ. Chem. Eng.*, 2020, **8**, 103912, DOI: 10.1016/j.jece.2020.103912.

52 A. Hidayat, W. K. Rochmadi, A. Nurdiawati, W. Kurniawan, H. Hinode, K. Yoshikawa and A. Budman, Esterification of palm fatty acid distillate with high amount of free fatty acids using coconut shell char based catalyst, *The 7th International Conference on Applied Energy-ICAE2015, Energy Procedia*, 2015, vol. 75 pp. 969–974, DOI: DOI: 10.1016/j.egypro.2015.07.301.

53 A. P. D. Correa, R. R. C. Bantos, G. N. D. Filho, J. R. Zamian and L. R. V. da Conceicao, Preparation of sulfonated carbon-based catalysts from murumuru kernel shell and their performance in the esterification reaction, *RSC Adv.*, 2020, **10**, 20245–20256, DOI: 10.1039/D0RA03217D.